

MIT Open Access Articles

*Efficient shRNA-Mediated Inhibition
of Gene Expression in Zebrafish*

The MIT Faculty has made this article openly available. **Please share**
how this access benefits you. Your story matters.

Citation: De Rienzo, Gianluca, Jennifer H. Gutzman, and Hazel Sive. "Efficient shRNA-Mediated Inhibition of Gene Expression in Zebrafish." *Zebrafish* 9.3 (2012): 97–107. ©2012 Mary Ann Liebert, Inc. publishers.

As Published: <http://dx.doi.org/10.1089/zeb.2012.0770>

Publisher: Mary Ann Liebert

Persistent URL: <http://hdl.handle.net/1721.1/74628>

Version: Final published version: final published article, as it appeared in a journal, conference proceedings, or other formally published context

Terms of Use: Article is made available in accordance with the publisher's policy and may be subject to US copyright law. Please refer to the publisher's site for terms of use.



Efficient shRNA-Mediated Inhibition of Gene Expression in Zebrafish

Gianluca De Rienzo,¹ Jennifer H. Gutzman,^{1,*} and Hazel Sive^{1,2}

Abstract

Despite the broad repertoire of loss of function (LOF) tools available for use in the zebrafish, there remains a need for a simple and rapid method that can inhibit expression of genes at later stages. RNAi would fulfill that role, and a previous report (Dong *et al.* 2009) provided encouraging data. The goal of this study was to further address the ability of expressed shRNAs to inhibit gene expression. This included quantifying RNA knockdown, testing specificity of shRNA effects, and determining whether tissue-specific LOF could be achieved. Using an F0 transgenic approach, this report demonstrates that for two genes, *wnt5b* and *zDisc1*, each with described mutant and morphant phenotypes, shRNAs efficiently decrease endogenous RNA levels. Phenotypes elicited by shRNA resemble those of mutants and morphants, and are reversed by expression of cognate RNA, further demonstrating specificity. Tissue-specific expression of *zDisc1* shRNAs in F0 transgenics demonstrates that conditional LOF can be readily obtained. These results suggest that shRNA expression presents a viable approach for rapid inhibition of zebrafish gene expression.

Introduction

PARAMOUNT TO UTILITY of the zebrafish is the ability to assay loss of function (LOF) phenotypes, and a wide array of techniques to perturb gene expression is available. Forward genetic screens have been very productive, using both chemical and insertional mutagenesis.^{1,2} Gene trapping has allowed tagging and mutagenesis,^{3,4} including an elegant conditional “protein trap” strategy.⁵ Inducible gene expression is possible using the Cre/lox system, Gal4/UAS lines, as well as doxycycline or tamoxifen-responsive promoters.^{6–8} Targeted LOF is achieved through TILLING,⁹ using zinc-finger nucleases^{10,11} or TALEN technology.^{12–14} In the embryo, stabilized morpholino-modified antisense oligonucleotides (MOs) can inhibit translation or splicing.¹⁵

Despite this battery of LOF techniques, there remains no reliable method to rapidly test LOF effects after embryonic stages, and in a tissue-specific fashion. Mutants have been identified only for a fraction of fish genes, and stage or tissue-specific loss of function is not generally possible. Antisense MO oligonucleotides (MOs) are quick to use, by injection into early embryos. However, MOs are diluted as the embryo grows, and their efficacy fades as they are diluted with cell division and embryonic growth. Further, MOs are expensive, may have poor solubility, and often give off-target effects.¹⁶ Photoactivatable MOs can be used later in development;

however, they are very expensive, and the frequency with which they can target a gene is not clear.^{17,18} Thus, there is a need for a rapid, inexpensive, tissue-specific method that can target specific genes in zebrafish beyond embryonic stages.

RNAi is an antisense-mediated process present in eukaryotic cells, whereby short hairpin RNAs (shRNAs), derived from longer double-stranded (ds) precursors, act post-transcriptionally to prevent expression of complementary RNA.¹⁹ Since long dsRNAs elicit an antiviral response and inhibit total translation, in order to use RNAi as a tool to inhibit gene expression, short hairpin RNAs (shRNAs) that do not elicit the antiviral response are employed. These are processed like endogenous miRNAs (Fig. 1), and can be expressed from DNA templates, to drive tissue-specific LOF. Thus, the Drosha enzyme processes double-stranded RNA to yield shRNAs, which are then cleaved into 21–22 bp fragments (siRNAs) by Dicer endonuclease. siRNAs enter the RNA-induced silencing complex (RISC), which mediates interaction of the antisense (guide) siRNA strand with the target. RISC includes Argonaute endonucleases that cleave target RNA if there is a complete match with the siRNA. RNAi prevents gene expression in many animals, including *Caenorhabditis elegans*, mouse, and *Drosophila*.^{20–22} Conditional RNAi in mouse, after injection of lentiviral constructs or using the Cre-lox system to control RNAi expression, is a popular

¹Whitehead Institute for Biomedical Research and ²Massachusetts Institute of Technology, Cambridge Massachusetts.

*Current address: University of Wisconsin—Milwaukee, Milwaukee, Wisconsin.

FIG. 1. shRNA expression from miR30-backbone vectors. (A) Schematic showing promoter-driven expression of shRNAs, where the hairpin sequence is cloned into the *miR30* backbone. After transcription, the priRNA is cleaved by Droscha to form an shRNA, which is further processed by Dicer into an siRNA and loaded into the RISC complex. The “guide” (antisense) strand then inhibits gene expression, leading to RNA cleavage if there is a complete match with the target. (B) Schematic of one construct employed. The *b-actin* promoter drives an actin-exon + intron construct including a *miR30*/shRNA cassette that is linked to a CFP reporter (pTolDest-bactin-actin/intron-miR30-CFP-pA). Nascent RNA is spliced and cleaved to yield shRNA and CPF, whose expression reflects extent of shRNA expression. (C) Extent of CFP expression in an F0 Tol2 transgenic embryo, using the construct shown in B. Lateral view, 24 hpf, head to top.

complement to targeted gene knockouts.^{23,24} An effective approach to optimize expression of targeting shRNAs is to replace the hairpin region of a miRNA gene with the targeting sequence.²⁵ The miRNA30 (*miR30*) backbone has been employed in mammalian tissue culture cells, and was chosen as it produces similar amounts of guide and passenger strands, perhaps allowing expression of shRNAs for many gene targets.²⁵ A similar strategy has been successful in *Drosophila*.²¹

The demonstration that RNAi can reliably target a significant number of genes would be welcome in the zebrafish community, since the regionalized functions of many genes could be readily explored during larval and adult stages. While it is not clear whether shRNAs would be properly processed during blastula stages due to limiting shRNA processing activity,²⁶ RNAi may be able to substitute for antisense MOs later. If targeting efficiency is high enough (perhaps 50%), it would be worthwhile, and feasible to produce a library of shRNA constructs targeting all or most zebrafish genes.

An elegant study from Dong *et al.*²⁷ showed that shRNAs injected into zebrafish embryos or expressed from the zebrafish *miR30* backbone could mediate RNAi. Assays in this study targeted an EGFP “sensor” or integrated transgene, or the endogenous *chordin* and *gata1* genes. Although results in this study were promising, RNA knockdown was not quantified, rescue of phenotypes with normal RNA was not performed, and tissue-specific LOF was not analyzed. To address these issues, we present a brief report of results obtained using shRNAs, expressed in an F0 transgenic assay, targeting the genes *wnt5b* and *zDisc1*, each with previously described morphant and mutant phenotypes.^{28–31} Our results add further support that shRNA-mediated LOF is an efficient mechanism to inhibit gene expression in the zebrafish.

Materials and Methods

shRNA design and purification

Hairpins for *zDisc1* and *wnt5b* were designed using Invitrogen Block-IT RNAi Designer software. Hairpin oligonucleotide pairs were purified by UREA-PAGE, annealed by heating to 95°C and slow cooling to 10°C. We have previously detailed these methods on ZFIN.⁴⁰ At least four hairpins per gene were tested. The guide strand siRNA sequence was designed to be a complete match to the target, which is anticipated to lead to cleavage of the target RNA after siRNA binding.¹⁹ When annealed, each hairpin contains a BbsI compatible site, for insertion into the *miR30* backbone.

Short hairpin sequences used

wnt5b ORF268for:

5'GGCTAGCCAACTCGTGGTTTGGTCATTACTGGTGCACATGATGGAGTAATGACCACCACGAGTTGGCC3'

wnt5b ORF268rev:

5'GGCTGGCCAACTCGTGGTGGTCATTACTCCATCATGTGCACCAGTAATGACCAAACCACGAGTTGGCT3'

wnt5b 3'UTR1299for:

5'GGCTAGGACAGACGCACCTTTGAGCAATTCTGGTGCAATGATGGAGAATTGCTCAGTGGCTGTGCTCC3'

wnt5b 3'UTR1299rev:

5'GGCTGGGACAGACGCACCTGAGCAATTCTCCATCATGTGCACCAGAATTGCTCAAAGTGGCTGTGCTCC3'

wnt5b 3'UTR1800for:

5'GGCTAGCAGGGTCTTTCTTGTATAGACGCTCTTAAGTGGTGCATGATGGAGTTAAGAGCGTCTATACGAAAGACCC3'

wnt5b 3'UTR1800rev:

5'GGCTGGGGTCTTTTCGTATAGACGCTCTTAAGTCCATCATGCACCAGTTAAGAGCGTCTATACAAGAAAGACCCCTGCT3'

FIG. 2. Inhibition of endogenous *wnt5b* expression. The 3'UTR1956 shRNA targeting *wnt5b* was expressed from an intronic *miR30* backbone, under the *b-actin* promoter, using the vector pTolDest-bactin-actin/intron-miR30-CFP-pA (see Materials and Methods). Transient transgenesis was induced using Tol2 transposase. (Aa) Vector schematic. (Ab) Relative expression of *wnt5b* mRNA after inhibition by shRNA. Expression was quantified by qPCR in 24 hpf embryos expressing the *wnt5b* 3'UTR1956 shRNA (*wnt5bh*) relative to embryos injected with a control hairpin (*YFP*). Data were normalized to endogenous *b-actin* RNA. (Ac) Northern blot analysis of RNA isolated from 24 hpf embryos demonstrating expression of the 21 base *wnt5bh* (antisense) guide strand (lane 1). The control is a synthetic *wnt5b* antisense strand DNA, run in parallel on the Northern blot (lane 2). (B) Whole mount *in situ* hybridization analysis of *wnt5b* expression in 12 hpf embryos expressing *YFP* (a, a') or *wnt5bh* (b, b') and in 24 hpf embryos expressing *YFP* (c) or *wnt5bh* (d). (a,b), dorsal views, anterior up; (a',b') lateral views, anterior up; (c,d) lateral views. (C) Phenotype of shRNA-expressing embryos and *wnt5b* morphants. (a-a'') 24 hpf control *YFP* embryos coinjected with *mcherry* RNA. (b-b'') 24 hpf *wnt5bh* embryos coinjected with *mcherry* RNA. (c-c'') 24 hpf *wnt5bh* embryos coinjected with *wnt5b* RNA. (d-d'') 24 hpf embryos injected with *wnt5b* MO together with the *p53* MO⁷ (see Materials and Methods). (a, b, c, d), lateral view of the head; (a', b', c', d'), dorsal view of the head after brain ventricle injection; (a'', b'', c'', d'') lateral view of whole embryo. (D) Whole mount *in situ* hybridization analysis of *myoD* expression in 12 hpf embryos expressing the following RNAs: *YFP* + *mcherry* RNA (a, a'), *wnt5bh* + *mcherry* RNA (b, b'), *wnt5bh* + *wnt5b* RNA (c, c') or injected with *wnt5b* MO (d-d'). Dorsal views. Black bracket: bent tail; white bracket: compressed somites.

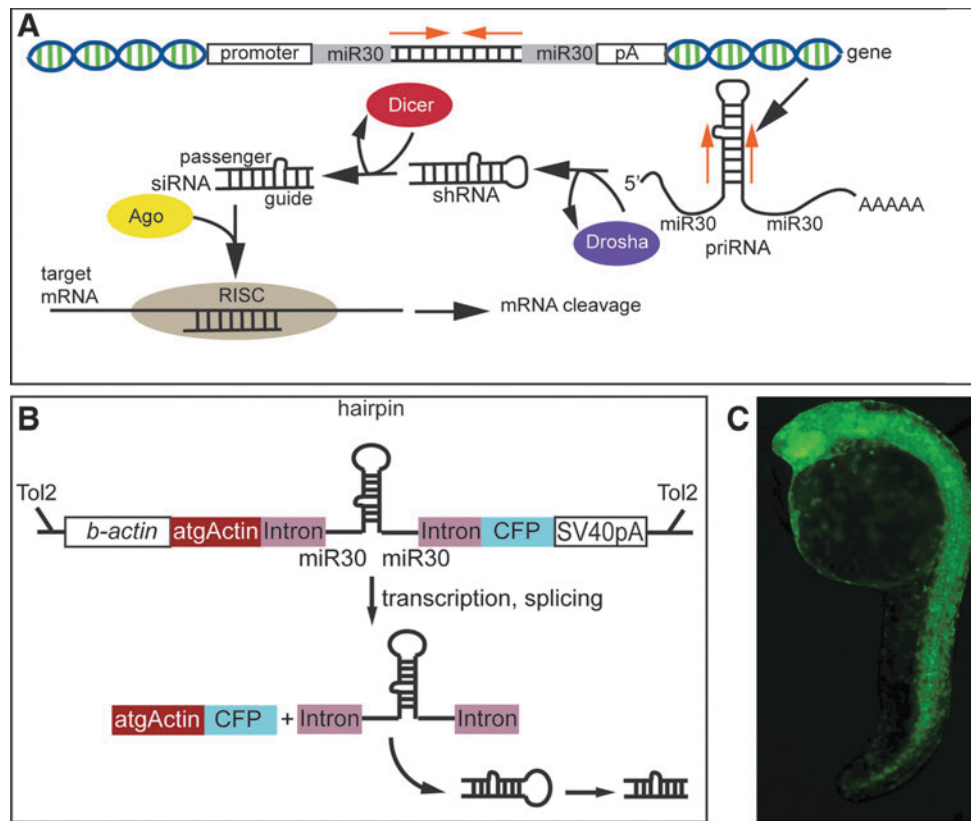


FIG. 1.

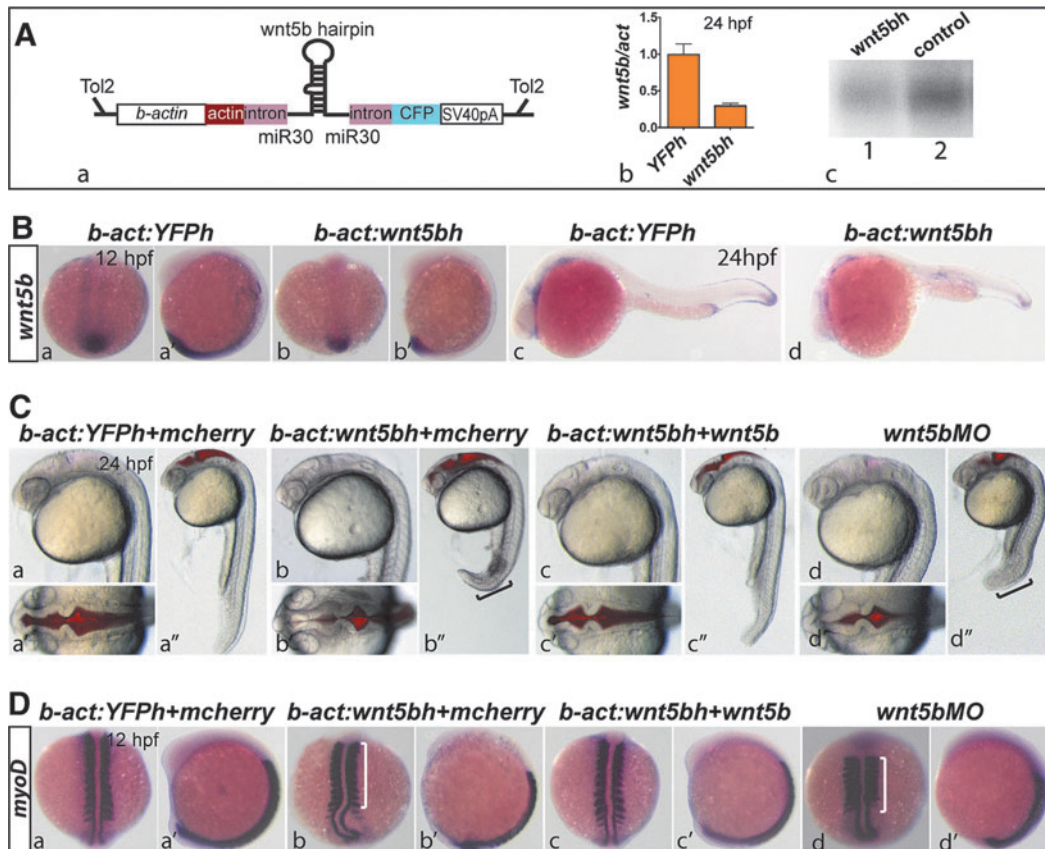


FIG. 2.

wnt5b 3'UTR1965for:

5'GGCTAGCACATAGAACCTTAGTGATCGCCAATTAAT
GGTGCACATGATGGAGTTAATTGGCGATCACTGGTTCT
ATGC3'

wnt5b 3'UTR1965rev:

5'GGCTGCATAGAACACAGTGATCGCCAATTAAGTCCAT
CATGTGCACCATTAATTGGCGATCACTAAGGTTCTATG
TGCT3'

zDisc1 ORF2247for:

5'GGCTAGCAGCAGTGCTATTAAGAGCTTAAGGCTGGT
GCACATGATGGAGCCTTAAGCTCTTAGCACTGCC3'

zDisc1 ORF2247rev:

5'GGCTGGCAGTGCTAAAGAGCTTAAGGCTCCATCATG
TGACCAGCCTTAAGCTCTTAATAGCACTGCTGCT3'

zDisc1 ORF2461for:

5'GGCTAGCAGCTTCTGGATTGGACAACTTCACTGGTG
CACATGATGGAGTGAAGTTTGTCTCCAGAAGCC3'

zDisc1 ORF2461rev:

5'GGCTGTGAAGTTTGTCTCCAGAAGCTCCATCATGT
GCACCAGTGAAGTTTGTCCAATCCAGAAGCTGCT3'

zDisc1 ORF2654for:

5'GGCTAGCAGCGCCATGTTTTGACTGCTTTAGCTGGTG
CACATGATGGAGCTAAAGCAGTCAACATGGCGCC3'

zDisc1 ORF2654rev:

5'GGCTGGCGCCATGTTGACTGCTTTAGCTCCATCATGT
GCACCAGCTAAAGCAGTCAAAACATGGCGCTGCT-3'

zDisc1 ORF2911for:

5'GGCTAGCAGGAGCTGAATTGTCTGCTCTTCACTGGTG
CACATGATGGAGTGAAGAGCAGACTTCAGCTCCC3'

zDisc1 ORF2911rev:

5'GGCTGGGAGCTGAAGTCTGCTCTTCACTCCATCATGT
GCACCAGTGAAGAGCAGACAATTCAGCTCCTGCT3'

As control we designed a hairpin targeting YFP (which is not expressed in the embryos used):

YFP ORF481for:

5'GGCTAGCAGCCACAACGTTTCTATATCATGGCTGGTG
CACATGATGGAGCCATGATATAGACGTTGTGGCC3'

YFP ORF481rev:

5'GGCTGGCCACAACGTTCTATATCATGGCTCCATCATGT
GCACCAGCCATGATATAGAAACGTTGTGGCTGCT

miR expression vector preparation

Two vectors were employed. The first, pTolDest-bactin-actin/intron-miR30-CFP-pA, included an actin-exon + intron-miR30 fragment. This fragment includes the first exon, including initiator ATG, and the first intron of the *b-actin* gene, with the zebrafish miR30 backbone inserted into the intron²⁷ (kind gifts from Dr. Ting Xi Liu). The miR backbone has a BbsI site into which the targeting short hairpin oligonucleotide is cloned. The actin-exon + intron-miR30 fragment was fused with the open reading frame of Cyan Fluorescent Protein (CFP) that lacks an initiator ATG, such that after transcription and correct splicing, the *b-actin* ATG is fused in frame to CFP. Expression of CFP therefore reflects correct splicing and indirectly, indicates shRNA expression. The "priRNA" produced after splicing, including the miR30 sequences and hairpin region is processed to yield the shRNA and then the siRNA (Fig. 1A). The actin-exon + intron-miR30-CFP fragment was cloned into the middle element (pme-MCF) plasmid from the Tol2 kit.³² The middle element and the p5E-bactin³² containing the *b-actin* promoter were assembled together with

pTolDestR4R2pA⁴¹ (that includes an SV40 poly A addition site) by LR reaction to create the expression GATEWAY vector pTolDest-bactin-actin/intron-miR30-CFP-pA.

Two other plasmids were used, I-SceI-mir124-miR30-GFP-pA and I-SceI-ntl-miR30-CFP-pA, containing I-SceI (meganuclease) target sites. In these, the CNS specific *mir124* promoter³⁵ or the meso-endoderm specific *no tail* (*ntl*) promoter³⁶ was cloned upstream of a GFP reporter followed by the zebrafish miR30 backbone, and of the SV40 poly A site. Hairpin oligonucleotides were inserted into the BbsI site of the miR30 backbone. Expression of GFP reflects transcription of the priRNA that can yield an shRNA.

Transgenic preparation

Transgenic analysis was performed in transient (F0) transgenics. For Tol2 constructs, 1 nl (25 pg) of a 25 ng/μl solution of each transgenesis vector was combined with 1 nl (25 pg) of a 25 ng/μl *Tol2* mRNA as described³² and injected into one-cell-stage eggs derived from the AB zebrafish strain. For meganuclease-based vectors, each construct (1 nl (30 pg) of a 30 ng/μl stock solution), together with 0.5 U of fresh I-SceI meganuclease (New England BioLabs), was injected into 1-cell fertilized embryos.

Quantitative RT-PCR (qPCR)

Total embryo RNA was extracted using Trizol (Invitrogen) followed by chloroform extraction and isopropanol precipitation and DNAase treatment or RNeasy kit (Qiagen). cDNA synthesis was performed with Super Script III Reverse Transcriptase (Invitrogen) and random hexamers. Primers for qPCR are:

zDisc1-for: 5'ATGAAGCCAACTCACAGCC3'
zDisc1-rev: 5'GTTTCTCCTTCATGCGGCTC3'
wnt5b-for: 5'ACCTACTTCTGGCAGTGACC3'
wnt5b-rev: 5'TTCCAGGTAATGCAGTCGGT3'
b-actin-for: 5'ATCAGGGTGTCATGGTTGGT3'
b-actin-rev: 5'CACGCAGCTCGTTGTAGAAG3'

qPCR was performed using a ABI Prism 7900 (ABI). Fluorescence detection chemistry utilized SYBR green dye master mix (Roche). The relative amount of product was calculated using $\Delta\Delta C_T$ and normalized to endogenous *b-actin* RNA. Values are reported with standard deviation. Each assay was performed in at least two independent experiments. Each experiment contained at least 40 CFP or GFP positive embryos per shRNA injected, which were divided into three, and separate RNA preparations performed for each set of embryos (biological replicates). Each RNA preparation was used for one reverse transcription reaction, which was then used in triplicate for each qPCR reaction (technical replicates).

Northern blot analysis

Northern blot analysis was performed as described.⁴² RNA from 30 embryos was loaded for each lane. A synthetic oligonucleotide complementary to the guide strand was 5' end-labeled with γ -³²P was used as probe. 100 pg of synthetic *wnt5b* or *zDisc1* antisense DNA was used as control.

Whole mount in situ hybridization analysis

For analysis of transcripts in the whole embryo, embryos were fixed in 4% PFA and *in situ* hybridization performed on 12 hpf or 24 hpf embryos, as described.⁴³ The *zDisc1* antisense

probe was prepared as published.³¹ The *wnt5b* antisense probe was prepared digesting pCS2-*wnt5b* plasmid, a kind gift from Dr. Diane Slusarski (University of Iowa), with BamHI and transcribing with T7 polymerase. The *myoD* antisense probe was prepared digesting pBluescript-*myoD* plasmid (a kind gift from Dr. Eric Weinberg [University of Pennsylvania]) with EcoRI and transcribing with T7 polymerase.

Microscopy

Methods for brightfield and fluorescence microscopy have been described previously.³⁸ Confocal imaging was performed on a Zeiss LSM710, after fixation in 2% TCA (acetylated α -tubulin) or 4% PFA (phalloidin).

Immunohistochemistry

Whole-mount immunostaining used mouse anti-acetylated α -tubulin (Sigma, 1:1000). Goat anti-mouse Alexa Fluor 488 (Molecular Probes, 1:500) was used as a secondary antibody. Staining by phalloidin Texas Red was performed as previously described.³¹

Brain ventricle injection and imaging

Brain ventricles were injected with Texas Red dextran, and superimposed brightfield and fluorescence imaging were performed as described previously.³³

RNA rescue assays

Capped RNA was synthesized using the Message Machine kit (Ambion), and injected at one-cell-stage. *hDisc1*, *wnt5b* and *mcherry* mRNAs were transcribed from pCS2-*hDisc1*,³¹ pCS2-*wnt5b* (very kindly provided by Dr. Diane Slusarski) and pCS2-*mcherry* (kindly provided by Dr. Frank Gertler [Massachusetts Institute of Technology]), respectively. For rescues, 200 pg (*zDisc1*) and 2 pg (*wnt5b* rescue) were injected, with an equivalent amount of *mcherry* RNA injected. Results obtained with or without injection of *mcherry* mRNA were indistinguishable.

Morpholino oligonucleotide injections

Antisense morpholino oligonucleotides (MOs; Gene Tools, LLC, Philomath, OR) were as follows: *zDisc1*MO, 5'-TCG CAGTTTTGTCTTACCTGTCTC-3'; *wnt5b*MO, 5'TGTTTAT TTCCTCACCATTCTTCC G- 3'; MO (1 nl) was injected into a single cell of a 1–2 cell embryo, using 3.5 ng for both *zDisc1* MO and *wnt5b* MO.^{16,31} For both *wnt5b* and *zDisc1*, a p53MO (5'GCGCCATTGCTTTGCAAGAATTG-3') was used at 1.5-fold greater than the mass of experimental MO to reduce off target effects.¹⁶

Fish embryos

Embryos were obtained from natural spawnings of an AB strain. Developmental stages are reported as hours post-fertilization (hpf) at 28°C. *Disc1fh291* mutants were isolated from a library of 8600 ENU-mutagenized F1 fish.^{31,44}

Results

We used two genes as tests of shRNA efficacy: *wnt5b* and *zDisc1*. For each gene, LOF phenotypes have been reported, with a similar phenotype is observed in both genetic mutants

and in morphants (i.e., after antisense morpholino-modified oligonucleotide injection). These phenotypes provide a basis for comparison with an shRNA-mediated phenotype. In these studies, shRNAs were expressed from a zebrafish miR30 backbone, with the cassette driven by a general or tissue-specific promoter, and tested in a transient (F0) transgenic assay (Fig. 1A and B). The assay was employed to rapidly test shRNA efficacies, and has the advantage that effects can be examined in the F0 (Fig. 1C). This type of analysis has the disadvantage of mosaicism, where fewer than 100% of cells become transgenic and express the shRNA, reducing the magnitude of shRNA effects. In order to overcome this disadvantage, we chose embryos expressing CFP extensively, and scored these for phenotypes. Each shRNA expression construct was assayed in at least two independent experiments, with total numbers of embryos examined indicated in the relevant section below.

shRNAs inhibit *wnt5b* expression effectively and specifically

The first gene targeted was *wnt5b*, considered a non-canonical *wnt*, which is expressed in the mesendoderm and tail bud. The LOF phenotype for *wnt5b* has been reported using antisense MOs^{16,30} and in the *pipetail* mutant *wnt5b*^{ti265/+}.^{28,29} A similar phenotype was obtained in both cases, namely, a bent tail, and associated abnormal convergence and extension.^{28,29} Four short hairpin sequences were designed to target *wnt5b* mRNA, that would bind both of the alternately spliced transcripts arising from this gene (Zv5–Zv9 releases, www.ensembl.org). shRNAs were cloned into the zebrafish miR30 backbone, in the pTolDest-bactin-actin/intron-miR30-CFP-pA vector, which is ubiquitously expressed from the *b-actin* promoter (Fig. 2Aa) (see Materials and Methods). F0 transgenic embryos were prepared using the Tol2 method,³² and examined at 24 hpf for a bent tail. One hairpin, mapping to 3'UTR in position 1956 gave a phenotype and this was used in subsequent assays. ORF269 and 3'UTR1299 hairpins also gave weaker phenotypes. F0 transgenic embryos were sorted for high CFP expression and harvested at 24 hpf for qPCR analysis, which showed an average of 71% ($n=5$ independent experiments, 82 total control and 78 total experimental embryos examined) decrease in *wnt5b* RNA after expression of the 3'UTR1956 *wnt5b* shRNA relative to a control YFP shRNA (Fig. 2Ab). Expression of the guide strand of the siRNA, which would bind to the *wnt5b* RNA target, was confirmed by northern analysis (Fig. 2Ac). A strong decrease in *wnt5b* RNA observed by qPCR was also seen by whole mount *in situ* hybridization analysis at 12 hpf and 24 hpf (Fig. 2B). Some RNA remained in both assays, possibly reflecting incomplete expression of the shRNA due to mosaicism, or targeting efficiency of the siRNA.

At 24 hpf, the effects of the *wnt5b* shRNA were monitored by examining embryos after injection of the brain ventricles with Texas Red dextran (Fig. 2Ca–b"). Brightfield and fluorescence images were superimposed to allow morphological examination of the brain, body and tail.³³ While expression of a control YFP shRNA did not significantly affect development ($n=81$, 86% normal embryos) (Fig. 2Ca–a"), after expression of the *wnt5b* shRNA, most embryos showed a short and bent tail ($n=74$, 19% normal embryos) (Fig. 2Cb", black bracket). This phenotype appeared identical to that observed after injection of *wnt5b* antisense MOs (Fig. 2Cd–d", $n=35$, 3% normal

FIG. 3. Inhibition of endogenous *zDisc1* expression. The ORF2654 shRNA (*zDisc1h*) targeting *zDisc1* was expressed in Tol2 F0 transgenic embryos, under control of the *b-actin* promoter, using the pTolDest-bactin-actin/intron-miR30-CFP-pA vector (see Materials and Methods). **(Aa)** Vector schematic. **(Ab)** Relative expression of *zDisc1* mRNA after inhibition by shRNA. Expression was quantified by qPCR in 24 hpf embryos expressing *zDisc1h* relative to embryos expressing a control shRNA, *YFP_h*. Data was normalized to endogenous *b-actin* RNA. **(Ac)** Northern blot analysis of RNA isolated from 24 hpf embryos demonstrating expression of the 21 base *zDisc1* (antisense) guide strand (lane 1). The control is a synthetic *zDisc1* antisense strand DNA, run in parallel on the Northern blot (lane 2). **(B)** Whole mount *in situ* hybridization analysis of *zDisc1* expression in 24 hpf embryos expressing *YFP_h* (a, a') or *zDisc1h* (b, b'). (a-b') Lateral views, anterior to the left; (a', b') higher magnification views. **(C)** Phenotype of shRNA-expressing embryos and *zDisc1* morphants and mutants. (a-a'') 24 hpf control *YFP_h* embryos coinjected with *mcherry* RNA. (b-b'') 24 hpf *zDisc1h* embryos coinjected with *mcherry* RNA. (c-c'') 24 hpf *zDisc1h* embryos coinjected with *hDisc1* RNA. (d-d'') 24 hpf embryos injected with *zDisc1* MO together with the *p53* MO⁷ (see Materials and Methods). (e-e'') 24 hpf *zDisc1*^{fh291} mutant embryos.³¹ (a, b, c, d, e), lateral view of the head; (a', b', c', d', e'), dorsal view of the head after brain ventricle injection; (a'', b'', c'', d'', e''), lateral view of whole embryo. **(D)** Forebrain neurons stained for acetylated tubulin in 36 hpf embryos expressing the following RNAs: *YFP_h* + *mcherry* RNA (a), *zDisc1h* + *mcherry* (b), *zDisc1h* + *hDisc1* (c), injected with *zDisc1* MO together with the *p53* MO (d) or *zDisc1*^{fh291} (e). Lateral views, anterior to left. **(E)** Muscle segments stained with phalloidin in 36 hpf embryos expressing the following RNAs: *YFP_h* + *mcherry* (a), *zDisc1h* + *mcherry* (b), *zDisc1h* + *hDisc1* (c), injected with *zDisc1* MO together with the *p53* MO (d) or *zDisc1*^{fh291} (e). Shape of muscle segments is indicated by dotted white lines. Black bracket: narrow brain ventricles; black asterisk: bent tail; black dotted lines: region between dotted lines was used for muscle segment analysis by phalloidin staining; ac, anterior commissure; poc, postoptic commissure; sot, supraoptic tract; tpc, tract of posterior commissure; white asterisk: defective supraoptic tract, region between dotted lines was used for muscle segment analysis by phalloidin staining.

embryos), and in the *pipetail* mutant,^{28,29} although the tail is shorter and the somites more compressed in morphant than in the mutant. In order to further test specificity of the shRNA-mediated phenotype, we asked whether injection of RNA encoding *wnt5b* could prevent the tail phenotype observed after shRNA expression, relative to injection of control *mcherry* mRNA. This RNA could not bind to the *wnt5b* RNA since it lacked the 3'UTR that the siRNA targeted, and prevented a tail phenotype in the siRNA-expressing fish. This indicated that the phenotype observed was specific and not due to off-target effects (*n*=29, 62% normal embryos) (Fig. 2Cc-c''). The *wnt5b* LOF phenotype and specificity was further explored by examining expression of *myoD* RNA that marks the developing somites, using *in situ* hybridization at 12 hpf (Fig. 2Da-c'). While expression of the *YFP* control shRNA did not alter somite formation (Fig. 2Da,a', *n*=15, 100% normal), after *wnt5b* shRNA expression, the somites were compressed (Fig. 2Db,b', white bracket, *n*=15, 20% normal embryos). This

indicates a convergence and extension abnormality, and was prevented by simultaneous injection of *wnt5b* RNA and the shRNA construct (Fig. 2Dc,c', *n*=15, 73% normal embryos). A similar *myoD* phenotype was observed in *wnt5b* morphants, although compression of the somites was more pronounced than after shRNA expression (Fig. 2Dd,d', white bracket, *n*=15, 13% normal embryos).

Together, these data indicate that expression of zebrafish *wnt5b* can be inhibited by shRNAs. Specificity of the phenotype was indicated by similarity to the published *pipetail* mutant and *wnt5b* morphant, and by the ability of cognate mRNA to prevent shRNA-associated phenotypes.

shRNAs target *zDisc1* effectively and specifically

The second gene targeted was *zDisc1*, for which we previously reported phenotypes of a morphant and a mutant, *Disc1*^{fh291}, demonstrating both brain, muscle segment, and

FIG. 4. Tissue-specific inhibition of *zDisc1* expression. The ORF2654 shRNA targeted to *zDisc1* (*zDisc1h*) was expressed in I-SceI (meganuclease)-derived F0 transgenic embryos, under control of the *mir124* or *ntl* promoter (see Materials and Methods). **(Aa)** Diagram of the I-SceI-mir124-miR30-GFP-pA vector, where shRNA expression is driven by the CNS-specific *mir124* promoter. **(Ab)** Relative expression of *zDisc1* mRNA after inhibition by shRNA. Expression was quantified by qPCR in 24 hpf embryos expressing *zDisc1h* relative to embryos expressing a control shRNA, *YFP_h*. Data was normalized to endogenous *b-actin* RNA. **(Ac)** Whole mount *in situ* hybridization analysis of GFP expression in in 48 hpf embryos expressing *zDisc1h*. **(B)** Phenotype of embryos expressing shRNA from the *mir124* promoter. (a-a'') 24 hpf control *YFP_h* embryos. (b-b'') 24 hpf *zDisc1h* embryos. (a, b), lateral view of the head; (a', b'), dorsal view of the head after brain ventricle injection; (a'', b''), lateral view of whole embryo. **(C)** Differentiated neurons stained for acetylated tubulin in 36 hpf embryos expressing *YFP_h* (a, b) or *zDisc1h* (c, d) under control of the *mir124* promoter. (a, c) lateral view of the head; (b, d) dorsal view of the hindbrain. **(D)** Muscle segments stained with phalloidin in 36 hpf embryos expressing *YFP_h* (a) or *zDisc1h* (b) under control of the *mir124* promoter. Shape of muscle segments is indicated by a dotted white line. **(Ea)** Diagram of the vector I-SceI-ntl-miR30-CFP-pA, driven by the mesoderm specific *ntl* promoter. **(Eb)** Relative expression of *zDisc1* mRNA after inhibition by shRNA. Expression was quantified by qPCR in 24 hpf embryos expressing the *zDisc1h* relative to embryos expressing the control shRNA, *YFP_h*. RNA levels were normalized to endogenous *b-actin* RNA. **(Ec)** Whole mount *in situ* hybridization analysis of CFP expression in in 24 hpf embryos expressing *zDisc1h*. **(F)** Phenotype of embryos expressing shRNA from the *ntl* promoter. (a-a'') 24 hpf control *YFP_h* embryos. (b-b'') 24 hpf *zDisc1h* embryos. (a, b), lateral view of the head; (a', b'), dorsal view of the head after brain ventricle injection; (a'', b''), lateral view of whole embryo. **(G)** Differentiated neurons stained for acetylated tubulin in 36 hpf embryos expressing *YFP_h* (a, b) or *zDisc1h* (c, d) under control of the *ntl* promoter. (a, c) forebrain neurons, lateral view, anterior to left; (b, d) dorsal view of hindbrain, anterior to top. **(H)** Muscle segments stained with phalloidin in 36 hpf embryos expressing *YFP_h* (a) or *zDisc1h* (b) under control of the *ntl* promoter. Shape of muscle segments is indicated by a dotted white line. Black bracket: narrow brain ventricles; black dotted lines: region between dotted lines was used for muscle segment analysis by phalloidin staining; black asterisk: bent tail; ac, anterior commissure; poc, postoptic commissure; sot, supraoptic tract; tpc, tract of posterior commissure; r, rhombomeres; white asterisk: defective supraoptic tract.

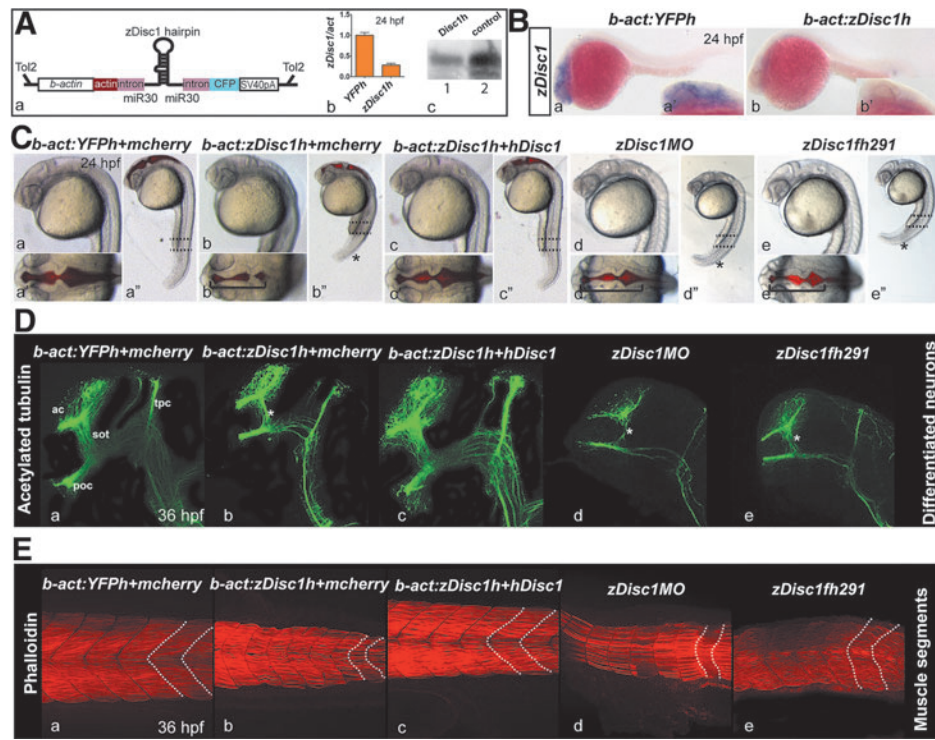


FIG. 3.

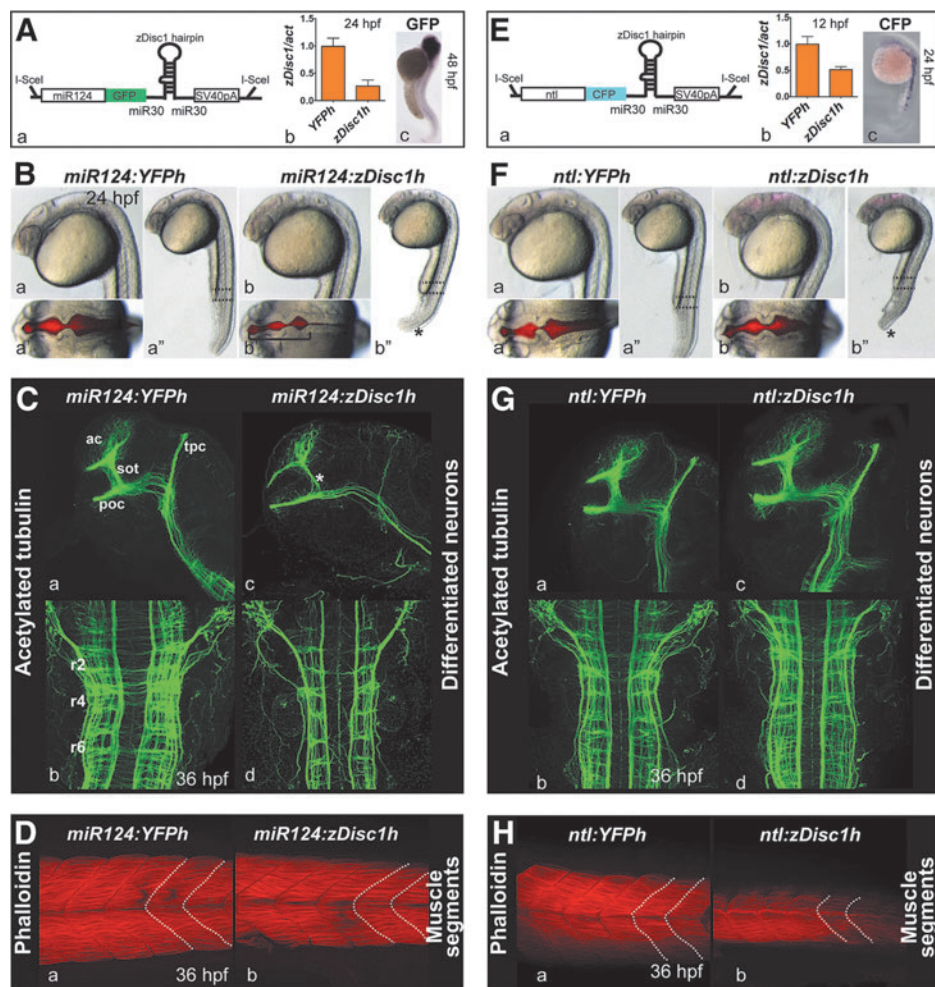


FIG. 4.

convergence and extension phenotypes.³¹ Similar to the strategy used to inhibit *wnt5b* expression, four short hairpins targeting *zDisc1* mRNA were designed and tested by expression from the *b-actin* promoter, using the pTolDest-bactin-actin/intron-miR30-CFP-pA vector (Fig. 3Aa; see Materials and Methods). Expression of two shRNAs targeting the open reading frame (ORF265 and ORF2911) in F0 transgenics resulted in a phenotype, while the others tested did not. The effect of the ORF2654 shRNA, which gave the strongest phenotype, was examined further. As shown by qPCR at 24 hpf, levels of *zDisc1* RNA were decreased by 70% on average ($n=8$ independent experiments, 138 total control and 129 total experimental embryos examined) (Fig. 3Ab). This decrease may reflect mosaic expression of the shRNA, or targeting efficiency of the siRNA. Consistent with shRNA-mediated targeting, the *zDisc1* siRNA guide strand was detected, by northern analysis (Fig. 3Ac). A decrease in *zDisc1* RNA levels was confirmed by *in situ* hybridization analysis at 24 hpf (Fig. 3B).

In comparison to embryos expressing the control YFP shRNA (Fig. 3Ca,a') ($n=124$, 79% normal), embryos expressing the *zDisc1* shRNA ORF2654 showed narrow brain ventricles and a truncated forebrain (Fig. 3Cb, b', black bracket) as well as a bent tail (Fig. 3Ca", b", black asterisk) ($n=84$, 19% normal embryos). This phenotype was prevented by injection of human *hDisc1* mRNA, which does not contain the siRNA target sequence, together with the Tol2 constructs (Fig. 3Cc-c") ($n=34$, 73% normal embryos), but not by injection of control *mcherry* mRNA. This result further demonstrates specificity of shRNA effects. The phenotypes observed in the *zDisc1* shRNA expressing embryos were similar to those we previously observed in the *zDisc1* morphant (Fig. 3Cd-d"; $n=159$, 6% normal) and mutant TILLED allele *Disc1*^{fh291} (Fig. 3Ce-e").³¹ This conclusion was further confirmed by examining forebrain axon tracts at 36 hpf, after staining with anti-acetylated α -tubulin. The supraoptic tract was reduced after *zDisc1* shRNA expression (Fig. 3Da,b, white asterisk) ($n=10$, 0% normal embryos), but not after control YFP shRNA expression ($n=10$, 100% normal). This tract is similarly thin in *zDisc1* mutants or morphants³¹ (Fig. 3Dd,e, white asterisk). The axon tract phenotype was prevented by injection of *hDisc1* RNA, but not by injection of *mcherry* mRNA, confirming specificity of the shRNA-mediated phenotype (Fig. 3Dc) ($n=10$, 90% normal embryos). Another characteristic phenotype after *zDisc1* LOF is presence of U-shaped muscle segments, likely linked to abnormal convergence and extension.³¹ Relative to YFP shRNA controls (Fig. 3Ea) ($n=10$, 100% normal), U-shaped muscle segments were observed at 36 hpf after expression of *zDisc1* shRNA, when segments were visualized by phalloidin staining (Fig. 3Eb) ($n=10$, 10% normal embryos). Abnormal muscle shape was prevented by injection of *hDisc1* mRNA together with the shRNA construct, but not by injection of *mcherry* mRNA (Fig. 3Ec), confirming specificity of the shRNA-mediated phenotype ($n=10$, 90% normal embryos). Similar phenotypes are observed for *zDisc1* mutant and morphant (Fig. 3Ed,e).³¹

Together, the data demonstrate that shRNAs can effectively mediate *zDisc1* LOF, resulting in a brain phenotype indistinguishable to that seen in the mutant, with a weaker brain phenotype than seen in the morphant. Muscle segment phenotypes were identical after shRNA expression to mutant and morphant.³¹ The rescue of these phenotypes by injected

hDisc1 RNA demonstrates specificity of shRNA effects and indicates that minimal off-target effects are associated with *zDisc1* shRNA expression.

Tissue-specific targeting of *zDisc1* expression

A key use for shRNAs in the zebrafish is to drive tissue-specific LOF, and so define the regional activities of a gene. Previous data, using *zDisc1* RNA specifically expressed in the CNS in a MO rescue assay, suggested that the axonal phenotype was associated with *zDisc1* activity in the neur ectoderm.³¹ In contrast, the muscle segment phenotype was associated with mesendodermal and, less so, with neur ectodermal activity also required for convergence and extension.^{31,34} We therefore tested the tissue-specific activities of *zDisc1*, by expressing the *zDisc1* ORF2654 shRNA from the CNS-specific *mir124* promoter³⁵ or the *ntl* promoter³⁶ that is active in the early mesendoderm and axial mesoderm (Fig. 4Aa, 4Ea).

After expression of *zDisc1* shRNA from the *mir124* promoter, *zDisc1* mRNA levels decreased by an average of 75% at 24 hpf (Fig. 4Ab) ($n=3$ independent experiments, 46 total control and 39 total experimental embryos examined). GFP expression, reflecting *mir124* promoter activity, was uniform in the CNS with no detectable ectopic expression (Fig. 4Ac). Relative to controls expressing YFP shRNA from the *mir124* promoter (Fig. 4Ba-a") ($n=84$, 93% normal), after expression of *zDisc1* shRNA, a brain and weak tail phenotype was observed (Fig. 4Bb-b") ($n=78$, 21% normal embryos). Forebrain and hindbrain axon tracts were thin when visualized with anti-acetylated α -tubulin at 36 hpf ($n=10$, 0% normal embryos) relative to normal tracts seen after YFP shRNA expression ($n=10$, 100% normal) (Fig. 4Ca-d). This is similar to the phenotype seen in the mutant and morphant,³¹ and after ubiquitous *zDisc1* shRNA expression (Fig. 3). These data are consistent with the majority of *zDisc1* expression in the brain and spinal cord. In contrast, muscle segments were normally shaped after neur ectodermal LOF (Fig. 4Da,b) ($n=10$, 100% normal embryos; as also observed after YFP shRNA expression: $n=10$, 100% normal).

Conversely, when *zDisc1* shRNA was expressed from the *ntl* promoter, a 50% average decrease in RNA levels, relative to total *b-actin*, was observed at 12 hpf, when *ntl* expression is maximal (Fig. 4Eb) ($n=3$ independent experiments, 51 total control and 49 total experimental embryos examined). This lower level of knockdown likely reflects residual expression of *zDisc1* in the developing brain that was not targeted by the *ntl* promoter. CFP *in situ* hybridization revealed expression specifically in the notochord, indicating localized *ntl* promoter activity (Fig. 4Ec). After *zDisc1* expression from the *ntl* promoter, brain morphology and axon tracts were indistinguishable from controls ($n=10$, 100% normal embryos; after expression of the YFP shRNA: $n=10$, 100% normal) (Fig. 4Fa,a',b,b' and Fig. 4G). In contrast, the tail was truncated ($n=63$, 22% normal embryos) relative to embryos after YFP shRNA expression ($n=75$, 87% normal) (Fig. 4Fa",b"). Consistently, thin and U-shaped muscle segments were observed (Fig. 4H) ($n=10$, 0% normal embryos) relative to effects of YFP shRNA expression ($n=10$, 100% normal). The data thus show a specific effect of the *zDisc1* shRNA on muscle segments when expressed in the mesendoderm.

These results indicate that *zDisc1* shRNAs can be successfully targeted to specific tissues to elicit local LOF phenotypes.

Discussion

We have demonstrated efficient targeting of two endogenous zebrafish genes using shRNAs, at mid- to late embryonic stages. The genes targeted are of interest in our laboratory, with described mutant and morphant phenotypes. The findings demonstrate that RNAi methodology works efficiently and specifically in the zebrafish, and add new shRNA reagents for functional analyses.

The results show for the first time in zebrafish, that shRNA expression can decrease RNA levels significantly, at least by 70% in mosaic F0 transgenic embryos. In mammalian cells, a 70% knockdown of endogenous RNA levels by transfected shRNAs is considered reasonable²⁵ (J. Doench and D. Root, Broad Institute, personal communication), and this LOF is clearly achievable in zebrafish. The siRNAs produced from the shRNAs most likely led to RNA cleavage, since the perfect match between siRNA guide strand and target used predicts RNA cleavage.¹⁹ Consistently, endogenous RNA levels decreased significantly. Additionally, qPCR using primers near the 5' end of the *zDisc1* gene or flanking the siRNA target site gave similar results, indicating that the entire RNA had been degraded (not shown). The F0 transgenic approach used to express the shRNAs is rapid and effective, but does give some mosaicism that may result in less than maximal LOF. In order to obtain uniform shRNA expression, inducible lines can be prepared. These may be necessary to allow viability after extensive LOF, and could use the Gal4/UAS strategy, or the various inducible Cre/lox approaches available.^{6,8} It seems very likely that inducible expression of shRNA can be achieved, but this remains to be tested.

The ability to prevent a phenotype by injection of cognate mRNA that does not bind the targeting siRNA, provided, for the first time, a stringent demonstration of specificity. The data further indicated that off-target effects of the shRNAs tested are small. In mammalian systems, rescue assays are generally not performed for shRNA-mediated LOF but are considered the "gold standard".³⁷ The zebrafish community established this stringent criterion to confirm MO specificity and we chose to require it of the shRNAs tested. Adopting this criterion for shRNAs would set a very high standard by the zebrafish community. For both *wnt5b* and *zDisc1*, phenotypes observed with the shRNA were not as severe as those seen in the morphant, which required p53 to suppress necrosis, but more like the mutant phenotype.³¹ This suggests that toxic effects of shRNAs may be generally lower than those observed with MOs.

shRNAs that were able to target the genes tested mapped to both the 3'UTR, which shRNAs traditionally target,¹⁹ and to the open reading frame (ORF). This indicates that in zebrafish, shRNAs can be designed to either part of the gene. While four hairpin sequences per gene tested yielded 2 per gene that elicited a phenotype, testing more (perhaps 6) per gene may give more efficient knockdown or may be necessary for some genes.

Many tissue-specific promoters have been identified in zebrafish and our demonstration of tissue-restricted effects of *zDisc1* shRNAs suggests that assaying shRNA effects in this way will be most useful. In these initial assays, we did not

examine effects of shRNA past 24 hpf, into later stages of organogenesis and function, and persistence of shRNA effects in larvae, juveniles, and adults, remains to be addressed.

What else has not been done in this analysis? We have not looked for phenotypes at blastula stages, because our test genes do not show a phenotype before the end of gastrulation. It is not clear whether shRNA processing activity (particularly Ago2) is limiting in the early zebrafish, as it appears to be in *Xenopus*,²⁶ and this will need to be tested. However, since MOs are effective in the early embryo, this activity is less critical than effectiveness of shRNAs in older embryos.

We do not have a large-scale measure of how frequently genes can be efficiently targeted by shRNAs. However, in our lab, we have successfully targeted 5 genes (of 6 tested) by shRNA expression (*wnt5b*, *zDisc1*, *aldoaa*, *kif22*, and *myoIIA*),^{31,38,39} although the extensive assays presented in this article have not yet been performed on some of these (HLS, unpublished, constructs available on request). In the Dong *et al*, 2009 study,²⁷ the *chordin* gene was targeted by shRNA injection and the *gata-1* gene was targeted by shRNA expression from the CMV promoter, but RNA quantification and rescue assays were not performed. Together, these data suggest that shRNAs may be able to target many genes in the zebrafish. However, a more extensive assessment of targeting efficiency and off-target effects will need to come from a future study.

In sum, we have presented results that support usefulness of shRNAs for zebrafish LOF analysis, suggesting that this approach could be used to develop an RNAi resource that would benefit the large group of researchers in the community.

Acknowledgments

This work was partially supported by NIH Grant R01 DE021109. Thanks to Sue-Jean Hong for help with northern blot analyses for siRNA detection. We thank members of the Sive lab for discussion and comments on the manuscript, especially Isabel Brachmann, Alicia Blaker-Lee, and Jasmine McCammon. Thanks to Olivier Paugois for expert fish husbandry, to David Root and John Doensch for helpful discussion, Jeong-Ah Kwon in the Genome Technology Core, and Nicki Watson in the Keck Imaging Facility. Thanks to Frank Gertler, Eric Weinberg, and Diane Slusarski for plasmids. We are grateful to Dr. Ting Xi Liu for an initial pCS2+actin-exon+intron-dsRed construct. Very sadly, Dr. Liu passed away last year, and his contributions to this field are respectfully acknowledged.

Disclosure Statement

No competing financial interests exist.

References

1. Haffter P, Granato M, Brand M, Mullins MC, Hammerschmidt M, Kane DA, *et al*. The identification of genes with unique and essential functions in the development of the zebrafish, *Danio rerio*. Development 1996;123:1–36.
2. Amsterdam A, Burgess S, Golling G, Chen W, Sun Z, Townsend K, *et al*. A large-scale insertional mutagenesis screen in zebrafish. Genes Dev 1999;13:2713–2724.
3. Amsterdam A, Becker TS. Transgenes as screening tools to probe and manipulate the zebrafish genome. Dev Dyn 2005; 234:255–268.

4. Balciunas D, Davidson AE, Sivasubbu S, Hermanson SB, Welle Z, Ekker SC. Enhancer trapping in zebrafish using the Sleeping Beauty transposon. *BMC Genomics* 2004;5:62.
5. Clark KJ, Balciunas D, Pogoda HM, Ding Y, Westcot SE, Bedell VM, *et al.* *In vivo* protein trapping produces a functional expression codex of the vertebrate proteome. *Nat Methods* 2011;8:506–515.
6. Scott EK. The Gal4/UAS toolbox in zebrafish: New approaches for defining behavioral circuits. *J Neurochem* 2009;110:441–456.
7. Hans S, Kaslin J, Freudenreich D, Brand M. Temporally-controlled site-specific recombination in zebrafish. *PLoS One* 2009;4:e4640.
8. Hans S, Freudenreich D, Geffarth M, Kaslin J, Machate A, Brand M. Generation of a non-leaky heat shock-inducible Cre line for conditional Cre/lox strategies in zebrafish. *Dev Dyn* 2011;240:108–115.
9. Moens CB, Donn TM, Wolf-Saxon ER, Ma TP. Reverse genetics in zebrafish by TILLING. *Brief Funct Genomic Proteomic* 2008;7:454–459.
10. Foley JE, Yeh JR, Maeder ML, Reyon D, Sander JD, Peterson RT, Joung JK. Rapid mutation of endogenous zebrafish genes using zinc finger nucleases made by Oligomerized Pool ENGINEERING (OPEN). *PLoS One* 2009;4:e4348.
11. Gupta A, Christensen RG, Rayla AL, Lakshmanan A, Stormo GD, Wolfe SA. An optimized two-finger archive for ZFN-mediated gene targeting. *Nat Methods* 2012;9:588–590.
12. Sander JD, Cade L, Khayter C, Reyon D, Peterson RT, Joung JK, Yeh JR. Targeted gene disruption in somatic zebrafish cells using engineered TALENs. *Nat Biotechnol* 2011;29:697–698.
13. Miller JC, Tan S, Qiao G, Barlow KA, Wang J, Xia DF, *et al.* A TALE nuclease architecture for efficient genome editing. *Nat Biotechnol* 2011;29:143–148.
14. Huang P, Xiao A, Zhou M, Zhu Z, Lin S, Zhang B. Heritable gene targeting in zebrafish using customized TALENs. *Nat Biotechnol* 2011;29:699–700.
15. Nasevicius A, Ekker SC. Effective targeted gene ‘knock-down’ in zebrafish. *Nat Genet* 2000;26:216–220.
16. Robu ME, Larson JD, Nasevicius A, Beiraghi S, Brenner C, Farber SA, *et al.* p53 activation by knockdown technologies. *PLoS Genet* 2007;3:e78.
17. Shestopalov IA, Sinha S, Chen JK. Light-controlled gene silencing in zebrafish embryos. *Nat Chem Biol* 2007;3:650–651.
18. Ouyang X, Shestopalov IA, Sinha S, Zheng G, Pitt CL, Li WH, *et al.* Versatile synthesis and rational design of caged morpholinos. *J Am Chem Soc* 2009;131:13255–13269.
19. Bartel DP. MicroRNAs: Target recognition and regulatory functions. *Cell* 2009;136:215–233.
20. Perrimon N, Ni JQ, Perkins L. *In vivo* RNAi: Today and tomorrow. *Cold Spring Harbor Perspect Biol* 2010;2:a003640.
21. Bakal C. *Drosophila* RNAi screening in a postgenomic world. *Brief Funct Genomics* 2011;10:197–205.
22. Azimzadeh Jamalkandi S, Masoudi-Nejad A. RNAi pathway integration in *Caenorhabditis elegans* development. *Funct Integ Genomics* 2011;11:389–405.
23. Scherr M, Battmer K, Ganser A, Eder M. Modulation of gene expression by lentiviral-mediated delivery of small interfering RNA. *Cell Cycle* 2003;2:251–257.
24. Kasim V, Miyagishi M, Taira K. Control of siRNA expression utilizing Cre-loxP recombination system. *Nucleic Acids Res Suppl* 2003;255–256.
25. Du G, Yonekubo J, Zeng Y, Osisami M, Frohman MA. Design of expression vectors for RNA interference based on miRNAs and RNA splicing. *FEBS J* 2006;273:5421–5427.
26. Lund E, Sheets MD, Imboden SB, Dahlberg JE. Limiting Ago protein restricts RNAi and microRNA biogenesis during early development in *Xenopus laevis*. *Genes Dev* 2011;25:1121–1131.
27. Dong M, Fu YF, Du TT, Jing CB, Fu CT, Chen Y, *et al.* Heritable and lineage-specific gene knockdown in zebrafish embryo. *PLoS One* 2009;4:e6125.
28. Hammerschmidt M, Pelegri F, Mullins MC, Kane DA, Brand M, van Eeden FJ, *et al.* Mutations affecting morphogenesis during gastrulation and tail formation in the zebrafish, *Danio rerio*. *Development* 1996;123:143–151.
29. Westfall TA, Brimeyer R, Twedt J, Gladon J, Olberding A, Furutani-Seiki M, Slusarski DC. Wnt-5/pipetail functions in vertebrate axis formation as a negative regulator of Wnt/beta-catenin activity. *J Cell Biol* 2003;162:889–898.
30. Kilian B, Mansukoski H, Barbosa FC, Ulrich F, Tada M, Heisenberg CP. The role of Ppt/wnt5 in regulating cell shape and movement during zebrafish gastrulation. *Mech Dev* 2003;120:467–476.
31. De Rienzo G, Bishop JA, Mao Y, Pan L, Ma TP, Moens CB, Tsai LH, Sive H. Disc1 regulates both β -catenin-mediated and noncanonical Wnt signaling during vertebrate embryogenesis. *FASEB J* 2011;25:4184–4197.
32. Kwan KM, Fujimoto E, Grabher C, Mangum BD, Hardy ME, Campbell DS, *et al.* The Tol2kit: A multisite gateway-based construction kit for Tol2 transposon transgenesis constructs. *Dev Dyn* 2007;236:3088–3099.
33. Gutzman JH, Sive H. Zebrafish brain ventricle injection. *J Vis Exp* 2009:1218.
34. Wallingford JB, Rowning BA, Vogeli KM, Rothbacher U, Fraser SE, Harland RM. Dishevelled controls cell polarity during *Xenopus* gastrulation. *Nature* 2000;405:81–85.
35. Shkumatava A, Stark A, Sive H, Bartel DP. Coherent but overlapping expression of microRNAs and their targets during vertebrate development. *Genes Dev* 2009;23:466–481.
36. Harvey SA, Tumpel S, Dubrulle J, Schier AF, Smith JC. No tail integrates two modes of mesoderm induction. *Development* 2010;137:1127–1135.
37. Echeverri CJ, Beachy PA, Baum B, Boutros M, Buchholz F, Chanda SK, *et al.* Minimizing the risk of reporting false positives in large-scale RNAi screens. *Nat Methods* 2006;3:777–779.
38. Gutzman JH, Sive H. Epithelial relaxation mediated by the myosin phosphatase regulator Mypt1 is required for brain ventricle lumen expansion and hindbrain morphogenesis. *Development* 2010;137:795–804.
39. Blaker-Lee A, Gupta S, McCammon JM, De Rienzo G, Sive H. Zebrafish homologs of 16p11.2, a genomic region associated with brain disorders, are active during brain development, and include two deletion dosage sensor genes. *Dis Model Mech* 2012 (e-pub ahead of print).
40. Gutzman JH, Sive H. RNAi for zebrafish. <https://wiki.zfin.org/display/prot/RNAi+for+Zebrafish> (posted to website July 13, 2010).
41. Villefranc JA, Amigo J, Lawson ND. Gateway compatible vectors for analysis of gene function in the zebrafish. *Dev Dyn* 2007;236:3077–3087.
42. Pall GS, Codony-Servat C, Byrne J, Ritchie L, Hamilton A. Carbodiimide-mediated cross-linking of RNA to nylon membranes improves the detection of siRNA, miRNA and piRNA by northern blot. *Nucleic Acids Res* 2007;35:e60.

43. Wiellette EL, Sive H. *vhnf1* and Fgf signals synergize to specify rhombomere identity in the zebrafish hindbrain. *Development* 2003;130:3821–3829.
44. Draper BW, McCallum CM, Stout JL, Slade AJ, Moens CB. A high-throughput method for identifying N-ethyl-N-nitrosourea (ENU)-induced point mutations in zebrafish. *Methods Cell Biol* 2004;77:91–112.

Address correspondence to:
Hazel Sive, Ph.D.
Massachusetts Institute of Technology
Nine Cambridge Center
Cambridge, MA 02142
E-mail: sive@wi.mit.edu